Nuclear Physics **A504** (1989) 456–466
North-Holland, Amsterdam

SIGNATURE INVERSION IN QUASIPARTICLE ENERGY AND B(M1)

Masayuki MATSUZAKI

Institute of Physics, University of Tsukuba, Ibaraki 305, Japan

Received 19 June 1989

Abstract: The signature inversion in quasiparticle energy and B(M1) is studied by means of the cranking model with fixed mean-field parameters. A qualitative explanation of the signature inversion in quasiparticle energy is given as the lowest-order response of rotating nuclei to a static triaxial field. The anomaly region, that is, the frequency region in which the signature inversion occurs in quasiparticle energy whereas the signature dependence of B(M1) is normal, is shown to exist systematically due to a specific phase relation between the single-particle matrix elements of quadrupole and angular-momentum operators at $\lambda \geq \epsilon_{3/2}$.

1. Introduction

The Coriolis force in rotating systems breaks the time-reversal invariance. Resulting new eigenstates of the cranking hamiltonian are classified by an eigenvalue r of the signature operation $R_x = \exp(-i\pi J_x)$. When the single-j approximation holds well and $j+\frac{1}{2}=$ even (odd), in odd-A nuclei the states with $r=+i(-i)$ usually lie lower in energy than their signature partners. This phenomenon is called the signature splitting. Henceforth we denote the energetically lowered state as the favoured (f) state and the other as the unfavoured (u) state. Magnetic-dipole transition rates between them also depend on the signature quantum number. Usually $B(\mathrm{M1}:\mathrm{f}\rightarrow\mathrm{u})$ is larger than $B(\mathrm{M1}:\mathrm{u}\rightarrow\mathrm{f})$. These rules hold in the nuclei with $\gamma \leq 0$ in the Lund convention except the three-quasiparticle band of ^{165}Lu [ref. [1]] (see sect. 3).

Based on the cranking model, Bengtsson *et al.* showed that the order of the f- and the u-states could be inverted in the nuclei with $\gamma > 0$ [ref. [2]] due to the shape driving force of another quasiparticle (see also ref. [3]). It was pointed out that the anti-alignment at $\hbar\omega_{\mathrm{rot}} \approx 0$ in such nuclei played an important role [4,5]) and that the particle-rotor model with the γ-reversed irrotational moment of inertia also gave the signature inversion [6–8]). These works have made it clear that the positive-gamma deformation is responsible for the signature inversion. But the qualitative mechanism of it at finite frequencies has not been fully understood yet.

Observed level energies of $(\pi \mathrm{h}_{11/2})^1(\nu \mathrm{i}_{13/2})^2$ states in the nuclei around $N=90$ show the signature inversion systematically but the behavior of B(M1) values depends on nuclide [9–17,1]). Therefore we should describe the signature inversion not only in quasiparticle energy but also in B(M1), which are related to each other, using a realistic framework which gives correct particle numbers in a high-j shell.

We performed such calculations including the quasiparticle-vibration-coupling effects previously using the self-consistent shapes given by the isotropic-velocity-distribution condition [18]). In this work, however, the calculated shapes β and γ were small and consequently we obtained almost no signature inversion (see sect. 4).

In the present paper, we propose an analytic explanation of the signature inversion in quasiparticle energy as the response of rotating nuclei to a static triaxial field. This is presented in a similar manner as in ref. [19]), in which the shell-filling dependence of the gamma-vibrational effects on B(E2: $\Delta I = 1$) has been clarified, and is suitable for the so-called Fermi-alignment (FAL) region [20]) (sect. 2). In sect. 3 an example of numerical calculation adopting a typical triaxial parameter is presented and the deviation of the signature-inversion frequency range of B(M1) from that of quasiparticle energy is studied analytically and numerically. The parameter dependence of the inversion range is discussed in sect. 4 as a basis for more elaborate calculations including the effects of the fluctuations of the nuclear shape and the rotational axis. The relation to the results presented in ref. [18]) is also discussed in this section. Concluding remarks are given in sect. 5.

2. A qualitative explanation of signature inversion

It was pointed out that the anti-alignment of the f-state at $\hbar\omega_{\rm rot} \approx 0$ caused by a positive-gamma deformation could be a source of the signature inversion [4,5]). But the anti-alignment can take place only instantaneously whereas the signature inversion appears irrespective of the alignment at $\hbar\omega_{\rm rot} \approx 0$ and persists up to high spins in realistic calculations with the pairing deformation. Therefore a more direct explanation which is suitable at finite rotational frequencies is desirable. In the following, we present a qualitative picture of the occurrence of the signature inversion and its shell-filling dependence in the nuclei at the FAL region, in which the angular-momentum projections onto both x- and z-axes are approximately good quantum numbers [20]), as the lowest-order response of rotating axially-symmetric nuclei to a triaxial field.

First of all, we review some relations between the single-particle matrix elements which have been shown to determine the shell-filling dependence of the gamma vibrational effects on B(E2: $\Delta I = 1$) [ref. [19])]. The cranking hamiltonian for axially-symmetric nuclei is written as

$$h' = h_{\rm sph} - \alpha_0 Q_0^{(+)} - \hbar\omega_{\rm rot} J_x \,. \tag{2.1}$$

From the commutators between h' and (J_z, iJ_y), we can derive the following identities:

$$\begin{aligned} -\Delta E\langle \mathrm{f}|J_z|\mathrm{u}\rangle &= \hbar\omega_{\rm rot}\langle \mathrm{f}|iJ_y|\mathrm{u}\rangle \,, \\ -\Delta E\langle \mathrm{f}|iJ_y|\mathrm{u}\rangle &= \hbar\omega_{\rm rot}\langle \mathrm{f}|J_z|\mathrm{u}\rangle + \sqrt{3}\alpha_0\langle \mathrm{f}|Q_1^{(-)}|\mathrm{u}\rangle \,, \end{aligned} \tag{2.2}$$

where the signature splitting of quasiparticle energy is defined by

$$\Delta E = E_{\mathrm{u}} - E_{\mathrm{f}} . \tag{2.3}$$

The quadrupole operators classified by the signature quantum number are given by

$$Q_K^{(\pm)} = \frac{1}{\sqrt{2(1+\delta_{K0})}} (Q_{+K} \pm Q_{-K}) , \tag{2.4}$$

and α_0 is a quadrupole deformation parameter. Using eqs. (2.2), we obtain the relation

$$\frac{\langle \mathrm{f}|Q_1^{(-)}|\mathrm{u}\rangle}{\langle \mathrm{f}|J_z|\mathrm{u}\rangle} = \frac{\hbar\omega_{\mathrm{rot}}}{\sqrt{3}\alpha_0} \left\{ \left(\frac{\Delta E}{\hbar\omega_{\mathrm{rot}}} \right)^2 - 1 \right\} . \tag{2.5}$$

This ratio is positive for the nuclei with low λ in a high-j shell since $|\Delta E|$ is larger than $\hbar\omega_{\mathrm{rot}}$ while it is negative for the nuclei with high λ (figs. 1 and 2 in ref. [19])). The quadrupole operators with $r=-1$ in a single-j shell model are represented by replacing the coordinate x by the angular momentum J [ref. [4])] as follows:

$$Q_1^{(-)} = -2\sqrt{3} c_{02} \tfrac{1}{2}\{J_x, J_z\} , \qquad Q_2^{(-)} = 2\sqrt{3} c_{02} \tfrac{1}{2}\{J_x, iJ_y\} , \tag{2.6}$$

with

$$c_0 = \sqrt{\frac{5}{16\pi}} \frac{q_0}{j(j+1)} , \tag{2.7}$$

where q_0 is a constant with dimension $[L^2]$. When the FAL picture is good, J_x in eqs. (2.6) can be replaced by an aligned angular momentum i_x and then

$$\frac{\langle \mathrm{f}|Q_2^{(-)}|\mathrm{u}\rangle}{\langle \mathrm{f}|Q_1^{(-)}|\mathrm{u}\rangle} \approx -\frac{\langle \mathrm{f}|iJ_y|\mathrm{u}\rangle}{\langle \mathrm{f}|J_z|\mathrm{u}\rangle} = \frac{\Delta E}{\hbar\omega_{\mathrm{rot}}} \tag{2.8}$$

holds well. Here the first equation of (2.2) is used. Consequently $\langle \mathrm{f}|Q_2^{(-)}|\mathrm{u}\rangle$ and $\langle \mathrm{f}|Q_1^{(-)}|\mathrm{u}\rangle$ have the same sign. (This holds in broad region of the parameter space even if γ is positive.) Namely, the phase rule (2.5) applies also to $\langle \mathrm{f}|Q_2^{(-)}|\mathrm{u}\rangle/\langle \mathrm{f}|J_z|\mathrm{u}\rangle$ (fig. 1 in ref. [19])).

Once the relative sign between $\langle \mathrm{f}|J_z|\mathrm{u}\rangle$ and $\langle \mathrm{f}|Q_2^{(-)}|\mathrm{u}\rangle$ is known, we can show the qualitative behavior of $\langle \mathrm{f}|Q_2^{(+)}|\mathrm{f}\rangle$ and $\langle \mathrm{u}|Q_2^{(+)}|\mathrm{u}\rangle$ since

$$\langle \mathrm{f}|Q_2^{(+)}|\mathrm{f}\rangle \approx -\langle \mathrm{u}|Q_2^{(+)}|\mathrm{u}\rangle \approx -\langle \mathrm{f}|J_z|\mathrm{u}\rangle\langle \mathrm{f}|Q_2^{(-)}|\mathrm{u}\rangle \tag{2.9}$$

is derived from the commutator between J_z and $Q_2^{(-)}$ assuming the FAL scheme, i.e. the matrix element $\langle \mathrm{f}|J_z|\mathrm{u}\rangle$ has non-zero values only between the signature-partner states. Schematic behavior of the matrix elements anticipated from eq. (2.9) is drawn in fig. 1. The most important point seen from it is that the sign of

$$\delta Q_2^{(+)} = \langle \mathrm{u}|Q_2^{(+)}|\mathrm{u}\rangle - \langle \mathrm{f}|Q_2^{(+)}|\mathrm{f}\rangle \tag{2.10}$$

changes at $\lambda_{\mathrm{crit}} \sim \varepsilon_{3/2}$. This holds also in realistic calculations (fig. 2).

The lowest-order response of rotating nuclei to a static triaxial field is determined by $\delta Q_2^{(+)}$. When a triaxial field $-\alpha_2 Q_2^{(+)}(\alpha_2/\alpha_0 = -\tan\gamma^{(\mathrm{pot})})$ is added to the hamiltonian h' (eq. (2.1)), an additional signature splitting $\delta E = -\alpha_2 \delta Q_2^{(+)}$ is produced. Therefore the signature inversion may occur as a result of the triaxial deformations

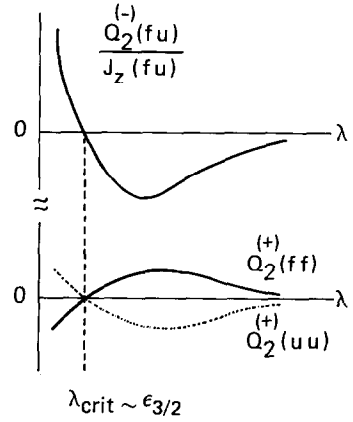

Fig. 1. A schematic drawing of the single-particle matrix elements as functions of the chemical potential in a high-j shell.

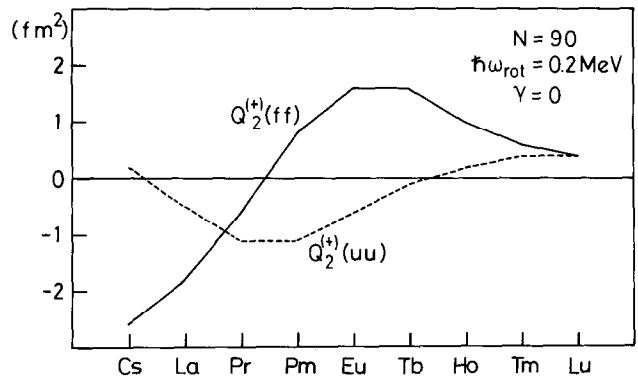

Fig. 2. Diagonal matrix elements of $Q_2^{(+)}$ for the yrast $(\pi h_{11/2})^1$ states at $\hbar\omega_{\rm rot} = 0.2$ MeV as functions of the proton number for the $N = 90$ isotones. The solid and the broken lines represent $\langle f|Q_2^{(+)}|f\rangle$ and $\langle u|Q_2^{(+)}|u\rangle$, respectively. Parameters used are $\beta^{(\rm pot)} = 0.20$, $\gamma^{(\rm pot)} = 0$, $\Delta_p = 1.0$ MeV and the chemical potentials which give correct particle numbers at $\hbar\omega_{\rm rot} = 0$ (the same as those adopted in ref. [19])).

$\alpha_2 \lessgtr 0$ in the nuclei with $\lambda \gtrless \lambda_{\rm crit}$. Since the normal signature splitting stemming from the cranking term is dominant in the low-λ region, the signature inversion can take place in the nuclei with $\gamma > 0$ and $\lambda > \lambda_{\rm crit}$. The additional signature splitting δE in such nuclei increases as $\hbar\omega_{\rm rot}$ increases but the normal signature splitting grows more rapidly. Consequently the signature inversion disappears at a certain $\hbar\omega_{\rm rot}$.

3. Deviation of signature-inversion frequency ranges of quasiparticle energy and B(M1)

It has been discussed by several authors that the signature dependence of not only energy spectrum but also electromagnetic transition rates is influenced by the γ-degree of freedom. It appears as the static deformation and the vibration. As for

the former, we should pay attention to the model dependence of its meaning. The one in the particle-rotor model is accompanied by the fluctuation of the rotational axis while in the cranking picture a triaxially-deformed potential rotates around a principal axis. At least a part of the effect of this fluctuation is taken into account by the quasiparticle-vibration coupling in our approach [21,18]). Namely, we can separate the effects of the triaxial deformation of a rotating potential itself and those of the fluctuations with various K. Static triaxial deformations magnify the rotational K-mixing in vibrational excitations in general. Fig. 2 in ref. [21]) illustrates the difference between the two in the case of $B(\mathrm{E2}: \Delta I = 1)$ within a one-quasiparticle (1 qp) band clearly. The fluctuation with $K = 2$ determines the signature dependence while the one with $K = 1$ influences the absolute value in the first order [19]).

In three-quasiparticle (3 qp) bands, the vibrational contributions become smaller than those in 1 qp bands because the collectivity of the K-mixed gamma-vibrations becomes weak in most cases [22]). This is consistent with the general expectation such that the cranking scheme becomes better at higher spins and/or for lower-Ω bands [compare fig. 8 in ref. [23]) and fig. 2 in ref. [21])]. But since the absolute magnitudes of the signature inversion in 3 qp bands are small, weak vibrational contributions may change the results of cranking calculations. An interesting example can be seen in the 3 qp band of ^{165}Lu; although the equilibrium γ-deformation is thought to be negative* because the neutron Fermi surface lies higher [24]), the signature inversion was observed [1]). This should be understood as an effect of the fluctuations. Therefore we should analyze such a phenomenon using the model which contains both the static deformation and the fluctuations around it. In the following, we discuss the result of a positive-gamma cranking calculation adopting a typical γ-deformation as a basis for the calculation including the effects of the fluctuations. We here aim at clarifying the relation between ΔE and $B(\mathrm{M1})$ in triaxial nuclei within the cranking model semi-quantitatively rather than fitting to the data. Results of the quasiparticle-vibration-coupling calculation based on the present work will be published separately.

Fig. 3 shows an example of numerical calculations with typical shape parameters. The parameters used in this calculation were fixed so as to reproduce the correct particule number and the average of observed $Q_t(2^+ \to 0^+)$'s of ^{158}Er and ^{160}Yb [ref. [25])] at $\hbar\omega_{\mathrm{rot}} = 0$ in the model space consisting of the three major shells** adopting $\Delta_p = 1.25$ MeV and $\gamma^{(\mathrm{pot})} = 15°$. Resulting signature splitting of quasiproton energy is common to the 1 qp and the 3 qp bands and is independent of the neutron part. A characteristic feature seen from this figure is that the signature inversion takes place in two regions. The inversion in low-frequency region is a direct result of the anti-alignment of the f-state at $\hbar\omega_{\mathrm{rot}} \approx 0$; this inversion region does not exist, for example, in the nuclei whose Fermi surfaces lie around $\varepsilon_{5/2}$ since the alignments

* The definition of the sign of γ in refs. [18,21,22,24]) is opposite to the Lund convention.

** The contributions of the lower N_{osc} shells were incorporated analytically in the same way as in ref. [24]).

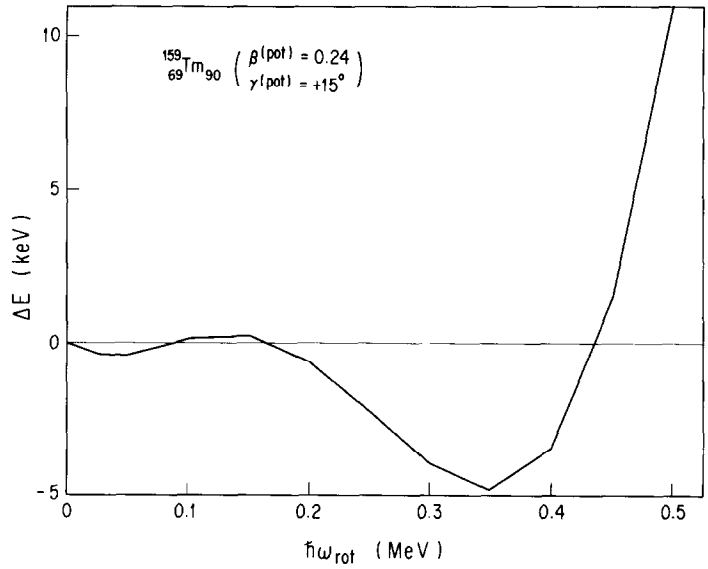

Fig. 3. Signature splitting of quasiparticle energy of the yrast sequence in ^{159}Tm as a function of the rotational frequency. These values are common to the 1 qp and the 3 qp bands. Negative values indicate the signature inversion. Parameter used are $\beta^{(pot)} = 0.24$, $\gamma^{(pot)} = 15°$, $\Delta_p = 1.25$ MeV and $\lambda_p = 5.871\hbar\omega_0$.

of their yrast f-states at $\hbar\omega_{rot} = 0$ are positive. This region ($\hbar\omega_{rot} < 0.1$ MeV) can not be detected experimentally and positive-gamma deformations are not adequate for the $(\pi h_{11/2})^1$ bands around $Z = 70$. The second (high-frequency) inversion region corresponds well to the observed one in the 3 qp band. But its maximum magnitude is smaller than the data [12-14]). In view of the previous calculation in which the fluctuations produced additional normal signature splitting in the positive-gamma 3 qp bands of $N = 90$ isotones [18]), larger γ-deformations will be necessary in order to fit to the data by the calculation including the vibrational contributions.

The probability distribution in the Ω-space is shown in table 1. As seen from it, there is almost no difference between the f- and the u-states. Therefore, the conjecture given by Ikeda and Åberg, such that different Ω-distributions due to the anti-alignment are responsible for the signature inversion [7]), does not seem a good explanation for the present situation where the proton Fermi surface lies around $\varepsilon_{7/2}$ and the pairing deformation is included. Since the axially-symmetric deformation energies of the signature-partner states, i.e. the diagonal matrix elements of $h_{sph} - \alpha_0 Q_0^{(+)}$ calculated with such wave functions, can be considered nearly the same, we can regard the total signature splitting simply as a sum of the normal contribution stemming from the difference in alignment and the opposite contribution stemming from $\delta Q_2^{(+)}$ in a good approximation. For example, $-\hbar\omega_{rot}\delta i_x$ is 23 keV and $-\alpha_2 \delta Q_2^{(+)}$ is -29 keV at $\hbar\omega_{rot} = 0.4$ MeV.

Fig. 4 shows the result for B(M1) calculated at the same time as ΔE in fig. 3. The neutron pairing gaps used in the calculation are 1.23 MeV for the 1 qp band

TABLE 1

Probability distribution of the favored and the unfavored yrast quasiproton states in ^{159}Tm. Parameters used are the same as those for fig. 3

$\hbar\omega_{rot}$ (MeV)	0	0.1	0.2	0.3	0.4	0.5
$f(r=+i)$						
$\Omega=\frac{1}{2}$	0	0.001	0.002	0.002	0.009	0.032
$\frac{3}{2}$	0.014	0.005	0.009	0.027	0.060	0.106
$\frac{5}{2}$	0	0.064	0.145	0.213	0.268	0.306
$\frac{7}{2}$	0.985	0.656	0.560	0.497	0.435	0.365
$\frac{9}{2}$	0	0.267	0.271	0.243	0.209	0.173
$\frac{11}{2}$	0.001	0.006	0.014	0.018	0.020	0.019
$u(r=-i)$						
$\Omega=\frac{1}{2}$	0	0.001	0.001	0.002	0.004	0.008
$\frac{3}{2}$	0.014	0.005	0.010	0.031	0.060	0.091
$\frac{5}{2}$	0	0.063	0.147	0.218	0.272	0.311
$\frac{7}{2}$	0.985	0.656	0.559	0.493	0.436	0.386
$\frac{9}{2}$	0	0.268	0.269	0.239	0.209	0.185
$\frac{11}{2}$	0.001	0.006	0.014	0.018	0.020	0.020

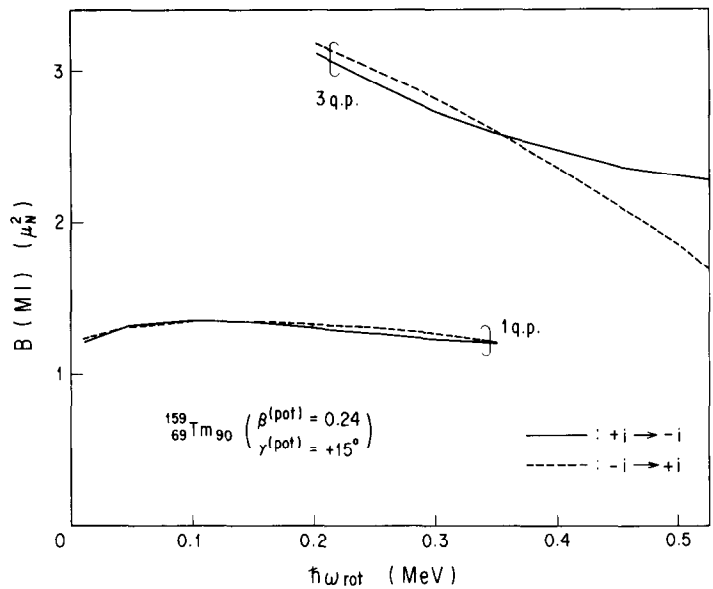

Fig. 4. B(M1) for the 1 qp and the 3 qp bands of ^{159}Tm. The solid and the broken lines represent the transitions from $r=+i$ and $r=-i$, respectively. Parameters used are $\Delta_n=1.23$ MeV for the 1 qp band and 0.86 MeV for the 3 qp band, respectively, $\lambda_n=6.403\hbar\omega_0$ and $g_s^{(eff)}/g_s^{(free)}=0.7$ for both bands and the others are the same as those for fig. 3.

and 0.86 MeV for the 3 qp band, respectively. The only influence of the band crossing on $B(\mathrm{M1})$ in this calculation appears via the change in the core g-factor (g_{RPA}) [refs. [21,18])]; the signature-inversion frequency range is independent of it and is common to both bands. The absolute magnitudes of $B(\mathrm{M1})$ in the 3 qp band are larger than the experimental values in ref. [14]). This discrepancy should be ascribed to the weak ω_{rot}-dependence of calculated g_{RPA} [ref. [26])]. Henceforth we concentrate on the signature dependence.

Corresponding to the behavior of ΔE, the signature dependence of $B(\mathrm{M1})$ is inverted in two regions. If the first equation of (2.2) holds, the signature-inversion range of $B(\mathrm{M1})$ coincides practically with that of ΔE since the matrix elements of M1 operator $\boldsymbol{\mu}$ are proportional to those of $\boldsymbol{J}$ in the single-j approximation. (As for the case of natural-parity bands, see ref. [27]).) In axially-asymmetric nuclei, however, the signature-inversion frequency ranges of ΔE and $B(\mathrm{M1})$ deviate from each other in general because another term is added to the equation as

$$-\Delta E\langle \mathrm{f}|J_z|\mathrm{u}\rangle = \hbar\omega_{\mathrm{rot}}\langle \mathrm{f}|iJ_y|\mathrm{u}\rangle + 2\alpha_2\langle \mathrm{f}|Q_2^{(-)}|\mathrm{u}\rangle\,. \tag{3.1}$$

In the present case, both the high-spin and the low-spin inversion regions shift to lower-frequency side. In particular, the signature dependence of $B(\mathrm{M1})$ is normal whereas the order of quasiparticle energies is inverted at $0.36 < \hbar\omega_{\mathrm{rot}} < 0.43$ MeV in accordance with the general trend of the data. We call this region the anomaly region. It may appear when $\langle \mathrm{f}|Q_2^{(-)}|\mathrm{u}\rangle/\langle \mathrm{f}|J_z|\mathrm{u}\rangle$ is negative. Therefore it will exist in the nuclei whose Fermi surfaces lie higher than λ_{crit} (see fig. 1 in ref. [19])). Its parameter dependence will be discussed in sect. 4.

When the FAL picture is good, anti-aligned f-states (and normally-aligned u-states) produce the signature inversion in $B(\mathrm{M1})$ since

$$\langle \mathrm{f}|J_x|\mathrm{f}\rangle \approx -\langle \mathrm{u}|J_x|\mathrm{u}\rangle \simeq -2\langle \mathrm{f}|J_z|\mathrm{u}\rangle\langle \mathrm{f}|iJ_y|\mathrm{u}\rangle \tag{3.2}$$

is derived from the commutator between J_z and iJ_y. Although the anti-alignment of the f-state occurs only instantaneously at $\hbar\omega_{\mathrm{rot}} \approx 0$ in realistic calculations, the frequency range in which the order of the aligned angular momenta is inverted ($\langle \mathrm{f}|J_x|\mathrm{f}\rangle < \langle \mathrm{u}|J_x|\mathrm{u}\rangle$) coincides well with the inversion range of $B(\mathrm{M1})$.

4. Parameter dependence of signature-inversion frequency range

The dependence of the signature-inversion frequency range of ΔE on mean-field parameters has been studied extensively by Bengtsson *et al.* [12]). We, therefore, concentrate our attention on the variation of the anomaly region in 3 qp bands. The dependence of the inversion ranges of ΔE and $B(\mathrm{M1})$ on $\gamma^{(\mathrm{pot})}$, $\beta^{(\mathrm{pot})}$, Δ_{p} and λ_{p} are shown in figs. 5–8. In each figure only one parameter was varied around the value adopted for figs. 3 and 4 and the others were fixed. We can see from these figures that the anomaly region exists irrespective of a special choice of mean-field parameters.

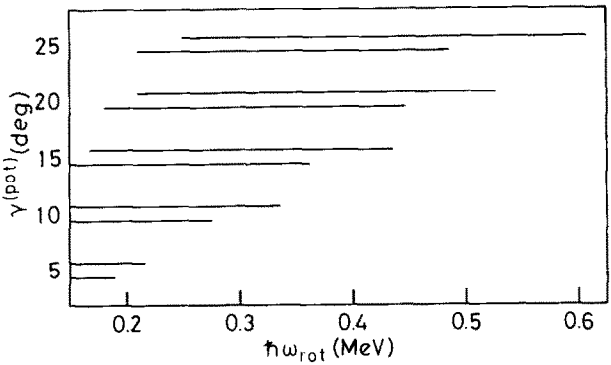

Fig. 5. The variation of the signature-inversion frequency range with $\gamma^{(pot)}$. The upper and the lower lines for each value indicate the inversion ranges of ΔE and $B(M1)$, respectively. Other parameters are the same as those for figs. 3 and 4.

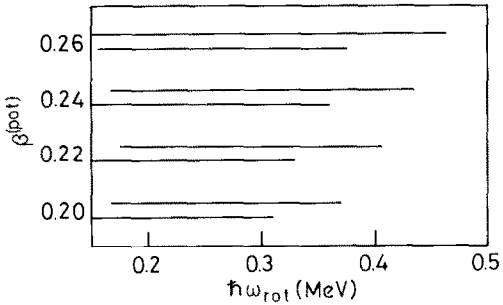

Fig. 6. The variation of the signature-inversion frequency range with $\beta^{(pot)}$. The upper and the lower lines for each value indicate the inversion ranges of ΔE and $B(M1)$, respectively. Other parameters are the same as those for figs. 3 and 4.

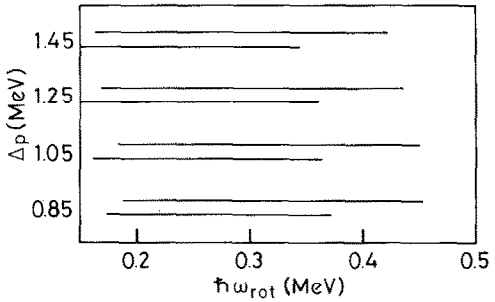

Fig. 7. The variation of the signature-inversion frequency range with Δ_p. The upper and the lower lines for each value indicate the inversion ranges of ΔE and $B(M1)$, respectively. Other parameters are the same as those for figs. 3 and 4.

The inversion range varies drastically with γ; it disappears practically for $\gamma^{(pot)} = 5°$ in the frequency region which corresponds to 3 qp bands. This is the main reason why we obtained almost no signature inversion in the previous calculation [18]). An interesting point seen from fig. 5 is that the anomaly region grows with γ since the

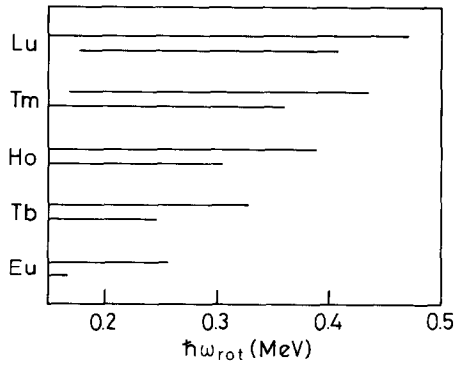

Fig. 8. The variation of the signature-inversion frequency range with proton number in the $\pi h_{11/2}$ shell. The upper and the lower lines for each nuclide indicate the inversion ranges of ΔE and $B(\mathrm{M1})$, respectively. Other parameters are the same as those for figs. 3 and 4.

second term in the right-hand side of eq. (3.1) prevents the $B(\mathrm{M1})$ from following the signature inversion in ΔE.

The inversion range grows as β increases (fig. 6) but the maximum magnitude of inversion (about 5 keV in the present case) is nearly independent of β. This presents a clear contrast to the fact that γ influences not only the frequency range of the inversion but also its depth. The smallness of calculated values for $\beta^{(\mathrm{pot})}$ is another reason why we obtained almost no signature inversion in ref. [18]).

The dependence on Δ_p is not strong but the inversion survives up to higher frequencies (fig. 7) and deepens as Δ_p decreases.

As proton number increases, the signature inversion survives up to higher frequencies (fig. 8) but its depth becomes shallow in accordance with the data. The former is due to the distance from the decoupling ($\Omega = \frac{1}{2}$) orbital whereas the latter is due to the magnitude of $\delta Q_2^{(+)}$ (fig. 2). In addition, the anomaly region enlarges at low λ_p because of the shell-filling dependence of $|\langle \mathrm{f}|Q_2^{(-)}|\mathrm{u}\rangle|$ (fig. 1 in ref. [19])). Neutron number will also influence the signature inversion in more elaborate calculations. Its effects appear indirectly via the change in equilibrium nuclear shapes and in properties of vibrational excitations.

5. Concluding remarks

We have studied the signature inversion in quasiparticle energy and $B(\mathrm{M1})$ analytically and numerically within the cranking model. A qualitative explanation of the signature inversion in quasiparticle energy has been given as the response of rotating nuclei to a static triaxial field utilizing the relations which determine the shell-filling dependence of the gamma-vibrational effects on $B(\mathrm{E2}: \Delta I = 1)$. This picture is suitable for the so-called Fermi-alignment region. The deviation of the signature-inversion frequency ranges of quasiparticle energy and $B(\mathrm{M1})$ has also been studied. The existence of the anomaly region, that is, the frequency region in

which the order of quasiparticle energies is inverted whereas the signature dependence of $B(M1)$ is normal, has been shown to originate from the λ-dependent phase relation between the single-particle matrix elements of $Q_2^{(-)}$ and J_z. Numerical calculations show that the anomaly region exist systematically in accordance with the general trend of the experimental data.

The present work within the cranking model gives a basis for the calculation including the effects of the fluctuations. Such calculation and quantitative comparison with the data and the particle-rotor-model calculation are in progress.

The author would like to express his thanks to Dr. Y.R. Shimizu for providing the computer code. This work was started at the Department of Radioisotopes, Japan Atomic Energy Research Institute and supported in part by the Grant-in-Aid for Scientific Research from the Ministry of Education, Science and Culture (No. 01790182). The author is indebted to Fellowships of the Japan Society for the Promotion of Science for Japanese Junior Scientists.

References

1) P. Frandsen *et al.*, Nucl. Phys. **A489** (1988) 508
2) R. Bengtsson *et al.*, Nucl. Phys. **A415** (1984) 189
3) S. Frauendorf and F.R. May, Phys. Lett. **B125** (1983) 245
4) I. Hamamoto and B. Mottelson, Phys. Lett. **B127** (1983) 281
5) N. Onishi and N. Tajima, Prog. Theor. Phys. **80** (1988) 130
6) I. Hamamoto and B. Mottelson, Phys. Lett. **B132** (1983) 7; I. Hamamoto, Annals of Israel Physical Society 7, 1984, p. 209
7) A. Ikeda and S. Åberg, Nucl. Phys. **A480** (1988) 85
8) A. Ikeda and T. Shimano, Phys. Rev. Lett. **63** (1989) 139
9) G.B. Hagemann *et al.*, Nucl. Phys. **A424** (1984) 365
10) D.C. Radford *et al.*, contribution to Workshop on nuclear structure, Copenhagen, 1988
11) M.A. Riley *et al.*, Proc. Conf. on high-spin nuclear structure and novel nuclear shapes, Argonne 1988, ANL-PHY-88-2, p. 211
12) A.J. Larabee *et al.*, Phys. Rev. **C29** (1984) 1934
13) R. Holzmann *et al.*, Phys. Rev. **C31** (1985) 421
14) J. Gascon *et al.*, Nucl. Phys. **A467** (1987) 539
15) C. Foin *et al.*, Nucl. Phys. **A417** (1984) 511
16) C.-H. Yu *et al.*, Nucl. Phys. **A489** (1988) 477
17) K. Honkanen *et al.*, Proc. 1986 American Chemical Society Meeting, p. 555
18) M. Matsuzaki, Y.R. Shimizu and K. Matsuyanagi, Prog. Theor. Phys. **79** (1988) 836
19) M. Matsuzaki, Nucl. Phys. **A491** (1989) 433
20) S. Frauendorf, Phys. Scr. **24** (1981) 349
21) M. Matsuzaki, Y.R. Shimizu and K. Matsuyanagi, Prog. Theor. Phys. **77** (1987) 1302
22) Y.R. Shimizu and K. Matsuyanagi, Prog. Theor. Phys. **72** (1984) 799
23) I. Hamamoto, Nucl. Phys. **A421** (1984) 109c
24) Y.R. Shimizu and K. Matsuyanagi, Prog. Theor. Phys. **71** (1984) 960
25) S. Raman *et al.*, At. Data Nucl. Data Tables **36** (1987) 1
26) Y.S. Chen, P.B. Semmes and G.A. Leander, Phys. Rev. **C34** (1986) 1935
27) M. Matsuzaki, Phys. Rev. **C39** (1989) 691